Mansoura Engineering Journal

Volume 32 | Issue 1 Article 6

12-7-2020

# Computational Investigation of Spray Heat Exchanger Performance.

Mohamed Mahmoud Awad
*Mechanical Power Engineering., Faculty of Engineering, Mansoura University., Mansoura., Egypt*

El-Sayed Negeed
*Atomic Energy Authority, Nuclear Research Center, Reactors Dept., Cairo., Egypt*

A. Mariy
*Atomic Energy Authority, Nuclear Research Center, Reactors Dept., Cairo., Egypt*

Mohamed Mahmoud Mahgoub
*Mechanical Power Engineering., Faculty of Engineering., El-Mansoura University., Mansoura., Egypt*

# Computational Investigation of Spray Heat Exchanger Performance

Mostafa M. Awad*, El-Sayed R. Negeed**, A. H. Mariy** and M. M. Mahgoub*

* Mansoura University, Faculty of Engineering, Mechanical Power Dept., Egypt.
** Atomic Energy Authority, Nuclear Research Center, Reactors Dept., Cairo.

**ملخص البحث**

**دراسة حسابية لمعاملات أداء المبادل الحرارى من النوع الرشاش**

تحسين معامل انتقال الحرارة مهم جدا لتصميم وعمل المبادلات الحرارية. وفى هذة الدراسة تم عمل نموزج نظرى لدراسة معاملات أداء المبادل الحرارى من النوع الرشاش. وتهدف الدراسة الى ايجاد معدل التبخير من الماء المتساقط على انبوبة افقية ساخنة و تحديد مدى تأثير مسافة السقوط على هذا المعدل وعلى فاعلية انتقل الحرارة. وعلاوة على ذلك فان تاثير حجم القطرات الساقطة وتوزيعها ودرجة حرارة السطح الساخن على معدل التبخير قد تم دراسته ايضا.

لمسافة سقوط معينة وباستخدام معادلات الكتلة وكمية الحركة والطاقة للقطرات الساقطة امكن حساب التغير فى سرعة القطرة وحجمها ودرجة حرارتها. وفى هذة الدراسة ايضا تم حساب سمك طبقة البخار المتكونة حول سطح الانبوبة الساخن ومعدل التبخير وفاعلية انتقل الحرارة. ان عملية انتقل الحرارة قد تم دراستها لعوامل متغيرة من عملية النذرير مثل: سرعة التذرير ( كمية الماء الساقط على وحدة المساحات من سطح الانبوبة) وتتغير فى المدى (من 1.2532 الى 1.5314 كجم/م$^2$ ثانية) ، حجم القطرة (وتتراوح من 128.4 الى 300 ميكرومتر ) ، سرعة القطرة (وتتراوح من 3 الى 7.43 م/ثانية) ، درجة تبريد الماء (وتتراوح من 70 الى 7 $^0$م).

وقد اظهرت النتائج ان معدل التبخير وفاعلية انتقل الحرارة تزداد بزيادة درجة حرارة السطح الساخن وبخفض سرعة القطرات وكذلك بخفض حجم القطرات. وقد وجد انه هناك مسافة سقوط معينة يحدث عندها اعلى معدل تبخير والتى تعتمد على ظروف التشغيل. وبمقارنة النتائج الحالية مع نتائج باحثين اخرين وجد انه يوجد توافق جيد بينهما وكان الفرق بينهما يتراوح من 4 الى 15%.

## Abstract

*Enhancement of the heat transfer coefficient is important for the design and operation of heat exchangers. In this study, a numerical model is built to investigate the performance of spray cooling heat exchanger as water is sprayed on a horizontal tube. The objectives of the study are to evaluate evaporation rate of the falling water film on a horizontal tube evaporator and obtaining the effect of the distance from the nozzle to the hot tube location on the evaporation rate and on heat transfer effectiveness. Moreover, the effect of droplet size distribution and the hot tube surface superheating temperature on the evaporation rate are also conducted.*

*For a certain distance from nozzle distributor to the hot tube surface and by using the equations of mass, momentum and energy of the sprayed droplets, the change on droplet velocity, droplet size and its temperature can be evaluated. Vapor film is created around the hot tube surface. In this study, the formed vapor layer thickness around the hot surface, evaporation rate and heat transfer effectiveness were also evaluated. The heat transfer characteristics are investigated at the considered ranges of the various spraying parameters such as: sprayed mass velocity (sprayed mass flow rate per the unit area of the test tube) which ranged from 1.2532 to 1.5314 kg/m$^2$.s, droplet size (ranged from 128.4 to 300 m), droplet velocity (ranged from 3 to 7.43 m/s ) and sprayed droplet subcooled (ranged from 70 to 7 °C).*

*The results show that, the evaporation rate and the heat transfer effectiveness are mainly increased by increasing the surface temperature. Also, the evaporation rate and the heat transfer effectiveness are increased by decreasing the droplet velocity. At high initial sprayed mass velocity, the evaporated mass flow rate and the heat transfer effectiveness are inversely proportional to the droplet size. There is an optimum distance from nozzle distributor to the tube surface location at which the maximum evaporated rate will occur.*

*The comparison between the obtained results and the results due to others shows a good agreement in which the difference between these results was ranged from 4 to 15%.*

Accepted March 11, 2007

**Nomenclature**

| | |
|---|---|
| $A_o$ | Test tube outer surface area, $m^2$ |
| a | Droplet cross-sectional area, $m^2$ |
| $C_D$ | Drag force coefficient, - |
| $C_p$ | Specific heat at constant pressure, $kJ/kg.K$ |
| $d_i$ | Droplet initial diameter, $m$ |
| d | Droplet diameter after a falling distance, $m$ |
| $d_n$ | Nozzle diameter, $m$ |
| $d_{de}$ | Droplet diameter at the tube surface edge, $m$ |
| D | Differentiation sign, - |
| $D_i$ | Test tube inner diameter, $m$ |
| $D_o$ | Test tube outer diameter, $m$ |
| $F_o$ | Fourier number, - |
| g | Acceleration due to gravity, $m^2/s$ |
| h` | Average heat transfer coefficient, $kW/m^2.K$ |
| h | Enthalpy, $kW/m^2.K$ |
| k | Thermal conductivity, $kW/m.K$ |
| $k_t$ | Test tube thermal conductivity, $kW/m.K$ |
| L | Test tube length, $m$ |
| LH | Latent heat for vaporization, $kJ/kg$ |
| m' | Mass flow rate, $kg/s$ |
| $m'_{ev}$ | Evaporation rate, $kg/s$ |
| n | Number of sprayed droplets, - |
| P | Pressure, $bar$ |
| $P_{spray}$ | Spray pressure, $bar$ |
| q | Heat flux, $kW/m^2$ |
| $Q_d$ | Transmitted heat from the heated tube surface per one droplet , $kW$ |
| $Q_t$ | Transmitted heat, $kW$ |
| $Q_w$ | Evaporation heat for one droplet, $kW$ |
| $r_b$ | Radius of flat bottom of the droplet, $m$ |
| $r_c$ | Radius of a concentric circle on the hot surface on which droplets falling inside it will be evaporated before they arrive to the surface edge, $m$ |
| Re | Reynolds number, - |
| $t_1$ | Sprayed water initial temperature, $K$ |
| $t_2$ | Droplet temperature after a falling distance, $K$ |
| $t_{leid}$ | Leidenfrost temperature, $K$ |
| T | Temperature, $K$ |
| $t_w$ | Temperature of the test tube outer surface, $K$ |
| u | Radial velocity of the vapor film, $m/s$ |
| $v_1$ | Sprayed droplet initial velocity, $m/s$ |
| $v_2$ | Droplet velocity after a falling distance, $m/s$ |
| $v_g$ | vapor velocity, $m/s$ |
| zz | Falling distance (vertical distance from the nozzles distributor to the test tube surface), $m$ |
| $zz_{max.}$ | Maximum falling distance at which the all sprayed droplets will fall to the tube surface, $m$ |

**Greek letters**

| | |
|---|---|
| $\alpha$ | Thermal diffusivity, $m^2/s$ |
| $\delta$ | Vapor layer thickness, $m$ |
| $\varepsilon$ | Surface emissivity, - |
| $\psi$ | Critical deflection angle, $deg.$ |
| $\varphi_n$ | nozzle angle, $deg.$ |
| $\theta_2-\theta_1$ | The contact time between vapor and the sprayed droplets, $s$ |
| $\mu$ | Dynamic viscosity, $N.s/m^2$ |
| $\nu$ | Kinematic viscosity, $m^2/s$ |
| $\sigma$ | Surface tension, $N/m$ |
| $\tau_{max.}$ | Life time of the droplet (the necessary time for the droplet to absorb enough heat for its complete evaporation), $s$ |
| $\tau_r$ | Duration of the droplet's Journey from the first collision to the surface edge, $s$ |
| $\Delta t_{sup}$ | Superheating (the difference between the hot surface temperature and the formed vapor saturation temperature), $K$ |
| $\Delta t_{sub}$ | Subcooling (the difference between the formed vapor saturation temperature and the sprayed water initial temperature), $K$ |

**Subscripts**

f Vapor film
t Total
g Vapor
zz Falling distance

**Abbreviations**

CR Contact ratio (the ratio between the sprayed mass flow rate in-contact with the tube surface and all of the sprayed mass flow rate).
HTE Heat transfer effectiveness (the ratio between the evaporation rate and the initial sprayed mass flow rate).

## 1. Introduction

The impact of a droplet onto a hot solid surface is a fundamental phenomena in a variety of different applications such as spray cooling in nuclear reactors during loss of coolant accident, nuclear reactor primary circuit pressurizer spray control, spray cooling in flash evaporators, spray cooling in cryogenic applications and quenching in iron and steel industry. An experimental correlation for the heat transfer effectiveness in the region associated with film on film boiling heat transfer impacting sprays was obtained by Yao [1]. In his study, the analysis of the impacting sprays was classified into two cases; dilute spray (negligible heat transfer due to interaction among droplets) and dense spray (significant interaction).

Delocrio and Choi [2] studied the interference between droplets upon the heat transfer surface during an impacting process. They classified the interference between droplets of an impacting spray into two types: spreading and impacting interference. Spreading interference refers to the contact between two droplets upon spreading resulting in a reduced diameter. Impacting interference refers to the contact between two droplets as one droplet and it impacts upon the other droplet while it resides on the hot surface. Ito [3] investigated experimentally the heat transfer mechanism of fog cooling. It was concluded that the evaporation heat transfer increases inversely with square root of droplet diameter and droplet velocity and it was also shown that the mass velocity and the surface superheating, $\Delta t_{sup}$, have strong effect on the evaporation heat transfer. Yao and Choi [4] studied experimentally the heat transfer of mono-dispersed vertically impacting sprays. It was shown that at low liquid flux, the film boiling heat transfer of an impacting spray is affected by the droplet size and velocity; however, at high liquid flux these effects become much less observable. In their study, the dominant parameter affecting the impacting spray heat transfer is the liquid mass flux.

The main objective of the present work is directed towards the evaluation of the boiling heat transfer coefficient and on the evaporation rate for spray cooling on a horizontal tube evaporator. The analytical investigation is directed towards studying the effect of droplet size, droplet velocity, droplet density, initial spray subcooled and the distance between the nozzle distributor and the tube surface on the heat transfer coefficient and the evaporation rate.

## 2. Mathematical model

A theoretical numerical model is built to investigate the performance of spray cooling of water spray on a horizontal tube. This model based on the following assumptions:

The droplet is nearly spherical except for the flat bottom part facing the hot surface, the subcooled water droplet is floating on the hot surface in a spherical state and where there is a thin vapor layer of uniform thickness, the spray is considered a dilute (neglecting interaction between the droplets), spattering effect on the hot surface is

very weak. the vapor-liquid interface at the bottom of the droplet is at the saturation temperature corresponding to the environmental pressure, all the droplets have the same diameter, intensive vaporization occurs at the vapor- liquid interface and the vapor flow between the droplet and the heat transfer is considered to be radically, axisymmetric, steady, laminar, viscous and incompressible, the radiation heat transfer from heating surface to the droplet is small and can be neglected, and the droplet horizontal velocity at the tube surface is constant and dependent on the radial location of the first collision.

The system can be divided into two regions as the following:

1.The region between the nozzles distributor and the upper tube surface.
2.The region around the test tube.

2.1. Governing equations for the region (1)

The droplet is exposed to many forces in the region between the liquid sheet and the tube surface, as shown in Fig. (1):

The gravitational force can be written as:

$$F_1 = \frac{g\pi d^3 \rho_w}{6} \quad (1)$$

The buoyancy force can be written as:

$$F_2 = \frac{\pi g d^3 \rho_g}{6} \quad (2)$$

The drag force can be written as:

$$F_3 = \frac{C_D \pi d^2 \rho_g (v_w - v_g)^2}{8} \quad (3)$$

The coefficient of drag force ($C_D$) can be calculated from the following relation (Tanaka drag law) by Linn et. al [6].

$$C_D = \frac{24}{Re_d} \quad \text{for } Re_d < 2$$

$$C_D = \frac{10}{Re_d} \quad \text{for } 2 < Re_d < 500 \quad (4)$$

$$= 0.44 \quad \text{for } 500 < Re_d < 10^5$$

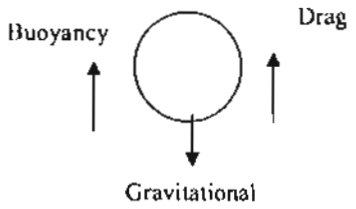


Fig. (1). Affecting forces on the droplet mitigation.

The momentum equation of the water droplet is written as:

$$m\frac{Dv}{D\theta} + v\frac{Dm}{D\theta} = \sum F \quad (5)$$

Where $\sum F$ is summation of effective forces on the droplet

i.e. $\Sigma F = F_1 - F_2 - F_3$ (6)

So, the momentum equation of the water droplet leaving the nozzle is written as:

$$\frac{\pi d^3 \rho_w Dv_w}{6D\theta} + \frac{(v_w - v_g)D(\frac{\pi}{6}d^3\rho_w)}{D\theta} = \frac{g\pi d^3\rho_w}{6} - \frac{\pi g d^3 \rho_g}{6} - \frac{C_D \pi d^2 \rho_g (v_w - v_g)^2}{8} \quad (7)$$

As comparing the vapor velocity with the sprayed water droplet velocity the vapor velocity is considered to be negligible, Ibrahim [5].

i.e. $v_g \approx 0.0$ then, equation(7) becomes:

$$\frac{Dv_w}{D\theta} = \frac{(\rho_w - \rho_g)g}{\rho_w} - \frac{3C_D\rho_g}{4\rho_w}\frac{v_w^2}{d} - \frac{v_w}{d^3}\frac{Dd^3}{D\theta} \quad (8)$$

The term $\frac{Dd^3}{D\theta} = 3d^2\frac{Dd}{D\theta}$, then equation (8) is reduced to:

$$\frac{Dv_w}{D\theta} = \frac{(\rho_w - \rho_g)g}{\rho_w} - \frac{3C_D\rho_g}{4\rho_w}\frac{v_w^2}{d} - \frac{3v_w}{d}\frac{Dd}{D\theta} \quad (9)$$

The change rate of droplet diameter ($\frac{Dd}{D\theta}$) can be obtained from

the following equation, Lekic and Ford [8]:

$$\frac{Dd}{D\theta} = \frac{2\pi^2 \alpha \varepsilon}{d_1} \frac{e^{-\pi^2 f_o}}{(1-e^{-\pi^2 f_o})^{1/2}} \quad (10)$$

where

$$\varepsilon = (1 + C_p(\frac{t_s - t_{w1}}{LH})^{1/3}) - 1 \quad (11)$$

$$\alpha = \frac{k_w}{\rho_w C_p} \quad (12)$$

$$f_o = \frac{4(\theta_2 - \theta_1)\alpha}{d_1^2} \quad (13)$$

The change of droplet diameter during condensation can be solved from the following equation, Lekic and Ford [8]:

$$d = d_1(1 + \varepsilon(1-e^{-\pi^2 f_o})^{\frac{1}{2}}) \quad (14)$$

By solving the equations (9), (10) and (14), then the rate of droplet velocity ($Dv_w/D\theta$) can be estimated in term of initial droplet diameter ($d_1$), initial droplet velocity ($v_1$), initial droplet temperature ($t_1$) and saturation temperature ($t_s$).

During the contact of water droplets with the vapor, heat is transferred between the two phases and droplet temperature ($t_2$) after distance ZZ from the nozzle distributor can be calculated from the following equation, Yuen et. al [7]

$$t_2 = \frac{1}{C_{p1}}(\frac{d_1^3(C_{p1}t_1 - h_s)}{d^3} + h_s) \quad (15)$$

where

The enthalpy of vapor ($h_s$) is a function of the evaporation pressure.

Due to the nozzle configuration the amount of contact ratio CR (the ratio between the sprayed mass flow rate in-contact with the tube surface and all the sprayed mass flow rate) changes as the distance ZZ increases. Thus the relation between the contact ratio CR at the distance ZZ and the maximum value of ZZ at which all the sprayed mass flow rate will fall to the tube surface will be analyzed in this section.

From figure (2) the following relation can be obtained

$$\sin(\frac{\psi_c}{2}) = \frac{\frac{D_o}{2}}{ZZ + \frac{D_o}{2}} \quad (16)$$

The maximum distance from the nozzle to the upper tube surface ($ZZ_{max.}$) occurs when the nozzle angle ($\varphi_n$) equal to the critical deflection angle ($\psi_c$), as shown in Fig. (2).

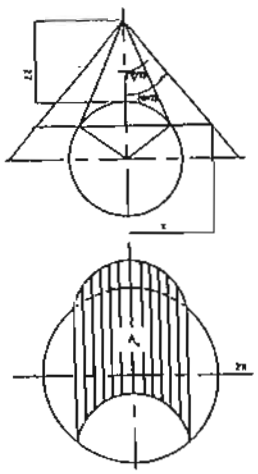

Fig. (2). Sprayed water droplets in-contact with the hot tube surface

Therefore: at $ZZ = ZZ_{max}$

then, $\psi_c = \varphi_n$

From equation (16);

$$ZZ_{max.} = \frac{\frac{D_o}{2}}{\sin(\frac{\varphi_n}{2})} - \frac{D_o}{2} \quad (17)$$

From Fig. (2), the surface area exposed to the sprayed droplets ($A_x$) can be calculated as,

$$A_x = ((\pi D_o \cos(\frac{\psi_c}{2}))\frac{2x}{2} \quad (18)$$

Equation (18) can be rewritten as:

$$A_x = \pi D_o x \cos(\frac{\psi_c}{2}) \quad (19)$$

From Fig. (2), the required surface area to make all the sprayed droplets fall to the tube ($A_t$) can be calculated as

$$A_t = \pi x^2 \quad (20)$$

The sprayed mass flow rate in contact with the tube is proportional to the falling area. Then, the mass flow rate for section zz can be written as:

$$m_{zz} = m_{w1}\frac{A_x}{A_1}c_3 \qquad (21)$$

where

$c_3$ is a fraction factor

$m_{w1}$ is all the sprayed mass flow rate

From equations (19), (20) and (21)

$$m_{zz} = m_{w1}\frac{D_o\cos(\frac{\psi_c}{2})}{x}c_3 \qquad (22)$$

As shown in Fig. (2)

$$x = \tan(\frac{\varphi_n}{2})(ZZ + \frac{D_o}{2} - \frac{D_o}{2}\sin(\frac{\psi_c}{2})) \qquad (23)$$

By substituting equation (23) in equation (22) then equation (22) can be rewritten as:

$$\frac{m_{zz}}{m_{w1}} = \frac{c_3 D_o\cos(\frac{\psi_c}{2})}{\tan(\frac{\varphi_n}{2})(ZZ + \frac{D_o}{2} - \frac{D_o}{2}\sin(\frac{\psi_c}{2}))} \qquad (24)$$

The boundary conditions are:

At $\varphi_n=\psi_c$, $ZZ=ZZ_{max}$,

then $m_{zz} = m_{w1}$ (25)

From equations (24) and (25), the constant $c_3$ can be obtained as:

$c_3 = ½$ (26)

By substituting equation (27) in equation (24) the sprayed mass flow rate in-contact with the tube can be calculated as:

$$m_{zz} = \frac{m_{w1}D_o\cos(\frac{\psi_c}{2})}{2\tan(\frac{\varphi_n}{2})(ZZ + \frac{D_o}{2} - \frac{D_o}{2}\sin(\frac{\psi_c}{2}))} \qquad (27)$$

and the contact ratio ($m_{zz}$ / $m_{w1}$) can be calculated as

$$CR = \frac{D_o\cos(\frac{\psi}{2})}{2(ZZ + \frac{D_o}{2} - \frac{D_o}{2}\sin(\frac{\psi}{2}))\tan(\frac{\phi_n}{2})} \qquad (28)$$

## 2.2. The region around the test tube

The total heat flux from the heated surface in the region associated with the film boiling ($q_t$), is assumed to be the sum of parallel contributions by radiation ($q_r$), convection ($q_c$) and evaporation ($q_w$), Yao [1].

$$q_t = q_r + q_c + q_w \qquad (29)$$

In the present study, water spray is achieved by pressure and compressed air not used, therefore the convective term of heat transfer can be neglected.

The radiation term of heat transfer is small and can be neglected when the surface superheating temperature is less than 300 °C, Yao [1].

Figure (3) shows a physical model of a single droplet in a spherical shape in which it is deflected from the tube surface by a thin vapor film. To calculate the vapor layer thickness (δ) and the transferred heat to a single droplet ($Q_d$), Baumeister and Hamil [9] developed a method, by solving the equations of momentum in the vapor layer, balance of energy at the liquid-vapor interface and balance of static forces exerting on a droplet simultaneously. The vapor layer thickness (δ) can be obtained as:

$$\delta = (\frac{9k_v\mu_v r_b^4\Delta t_{sup.}}{g\rho_l\rho_v d^3 L'})^{1/4} \qquad (30)$$

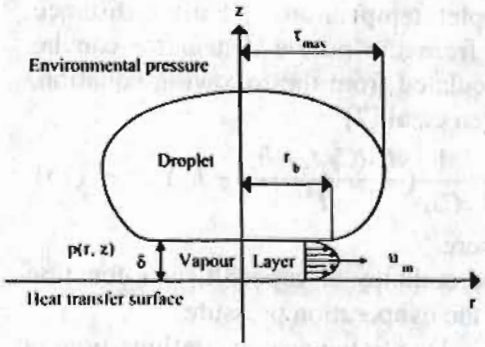


Fig. (3). Model of droplet evaporation.

where

$$\Delta t_{sup.} = t_w - t_s \qquad (31)$$

$r_b$ is radius of the flat bottom as a function of the diameter of the equivalent spherical droplet (d), $r_b$= 0.612 d

The transmitted heat to one droplet is introduced as:

$$Q_d = 1.11\left(\frac{g\rho_l\rho_v L' d_2^7 k_v^3 \Delta t_{sup.}^3}{\mu_v}\right)^{1/4} \quad (32)$$

The average heat transfer coefficient per droplet (h') can be introduced as:

$$h' = \frac{Q_d}{A_o \Delta t_{sat.}} \quad (33)$$

$$A_o = \pi L D_o \quad (34)$$

From equation (32), (33) and (34), then the average heat transfer coefficient per droplet (h') can be written as:

$$h' = \frac{1.11}{\pi L D_o}\left(\frac{g\rho_l\rho_v L' d_2^7 k_v^3}{\Delta t_{sat.}\mu_v}\right)^{1/4} \quad (35)$$

As the droplets fall from the nozzles distributor to the tube surface, portions of these droplets evaporate immediately as they contact with the surface, however, the other portions of droplets do not evaporate and reach to the tube edge.

Transferred heat from the entire heat transfer surface to the impinging droplets ($Q_w$) can be calculated from the following equation, Ito [10]

$$Q_w = n_a Q_d \tau_{max} 2\pi r_c L + \frac{\pi}{k}\int_{r_c}^{D_o/2} nQ_d L\left(\frac{D_o}{r} - 2\right) D(r) \quad (36)$$

where

$$n_a = n/(\pi D_o L) \quad (37)$$

and this transferred heat can be written as:

$$Q_w = n\, Q_d\, \tau_m \quad (38)$$

By using the energy equation describing the evaporation process of the droplet, life time of a droplet ($\tau_{max.}$) can be calculated as the following equation:

$$\tau_{max} = \frac{\pi d^3 \rho_l (C_{pl}\Delta t_{sub} + LH)}{6Q_d} \quad (39)$$

Figure (4) shows the journey of the droplet from the nozzle to the tube surface till to the tube edge.The horizontal droplet velocity (u) is assumed to be constant and dependents only on the radial location of the first collision, then

$$u = k\, r \quad (40)$$

where

k is constant which can be calculated with assuming the droplet size is constant.

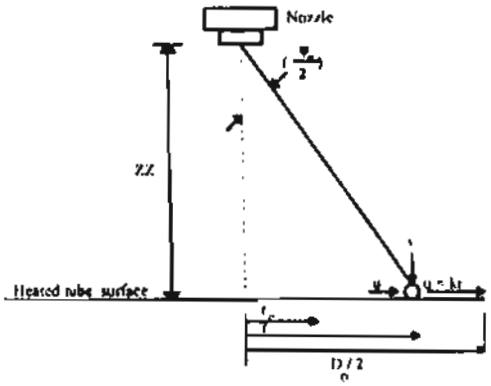


Fig. (4). Model of droplet behavior at and after collision.

Due to Lin and Ayyaswamy [11], the equation of droplet velocity can be written in differential from as:

$$\frac{Dv_w}{D\theta} = \frac{d^2}{4v_1 v_v}\left(\frac{R^2 g}{v_1 v_v} - \frac{3\rho_v}{16\rho_w} Pe_v C_{Dw} \frac{v_{w r}}{v_1}\cos\left(\frac{\varphi_w}{2}\right)\right) \quad (41)$$

$$\frac{Du_w}{D\theta} = \frac{d^2}{4v_1 v_v}\left(-\frac{3\rho_v Pe_v C_{Dw} v_{w\,r} \sin\left(\frac{\varphi_w}{2}\right)}{16\rho_w v_1}\right) \quad (42)$$

$Pe_v$ is Peclet number which can be written as:

$$Pe_v = \frac{v_{w\,r} 2R}{v_v} \quad (43)$$

$$v_{w\,r}^2 = (u_w^2 + v_w^2)^{1/2} \quad (44)$$

A general method to solve ordinary differential equations is by applying integration technique. The Runge - Kutta method is used to solve equations (41) and (42) and by applying the equation (40), then the constant (k) can be calculated, El-Sayed [12].

The time consumed by the un-evaporated droplet to move on the tube surface to the surface edge ($\tau_r$) can be calculated as:

$$\tau_r = \frac{\frac{D_o}{2} - r}{kr} \quad (45)$$

From the definitions of $r_c$ and $\tau_{max.}$, the following boundary conditions can be obtained:

At $r = r_c$ then, $\tau_r = \tau_{max.}$ (46)

and therefore,

$$r_c = \frac{D_o}{2(\tau_{max.} k + 1)} \quad (47)$$

By substitution equations (37), (45) and (47) in equations (36) and (38) then, the mean life time ($\tau_m$) can be introduced as:

$$\tau_m = \frac{1}{k} \ln(\tau_{max.} k + 1) \quad (48)$$

The transmitted heat flux from the heated surface to the droplets ($q_w$) can be calculated as:

$$q_w = \frac{nQ_d \tau_m}{\pi D_o L} \quad (49)$$

The evaporation rate, $\dot{m}_{ev.}$, can be calculated from the energy equation as:

$$\dot{m}_{ev.} = \frac{Q_w}{C_P \Delta t_{sub.} + LH} \quad (50)$$

Where

$$\Delta t_{sub.} = t_s - t_1 \quad (51)$$

The latent heat of evaporation (LH) is a function of the evaporation pressure.

The required heat to evaporate the all sprayed droplets ($Q_r$) can be calculated as:

$$Q_r = \dot{m}_{w1}(C_P \Delta t_{sub.} + LH) \quad (52)$$

The heat transfer effectiveness (HTE), which is the ratio between the transmitted heat from the heated surface ($Q_w$) to the required heat for evaporating all the sprayed droplets ($Q_r$) can be calculated as:

$$HTE = \frac{nQ_d \tau_m}{\dot{m}_{w1}(C_P \Delta t_{sub.} + LH)} \quad (53)$$

## 3. Results and discussions

The droplet size, droplet velocity and the contact ratio are changed by increasing the falling distance (ZZ). In this discussion, the effect of these changeable parameters on the evaporation rate and on the heat transfer effectiveness will be discussed.

### 3.1. Effect of the falling distance on the evaporation rate and on the heat transfer effectiveness

Figure (5) illustrates the effect of change of the falling distance (ZZ) on the sprayed droplets characteristics.

Figure (5a) illustrates the increase of the droplet size (d) obtained from equation (14) by increasing the falling distance (ZZ). That is due to the condensation of vapor on the droplet surface.

Figure (5b) illustrates the decrease of the droplet velocity ($v_2$) against the falling distance (ZZ). The decrease in the droplet velocity is due to the effects of drag and buoyancy forces produced from the formed vapor.

Figure (5c) illustrates the change of the contact ratio (CR) obtained from equation (28) with the falling distance. From the figure, it can be seen that, there is a maximum value of ZZ at which all the sprayed droplets fall on the tube surface. After this value, increasing the falling distance decreases the contact ratio.

Figure (5d) illustrates, the increase of the waiting time ($\tau_m$) obtained from equation (48) with increasing the falling distance (ZZ). This is due to the following two effects occur by increasing the falling distance

1. The droplet size increases, as shown in Fig. (5a), which allows a large effecting area exposed to the heating surface and hence, a more heat for evaporation is required, so the waiting time will increase.
2. The droplet velocity decreases, as shown in Fig. (5b), thus the droplet horizontal velocity on the tube surface decreases, so the waiting time will increase.

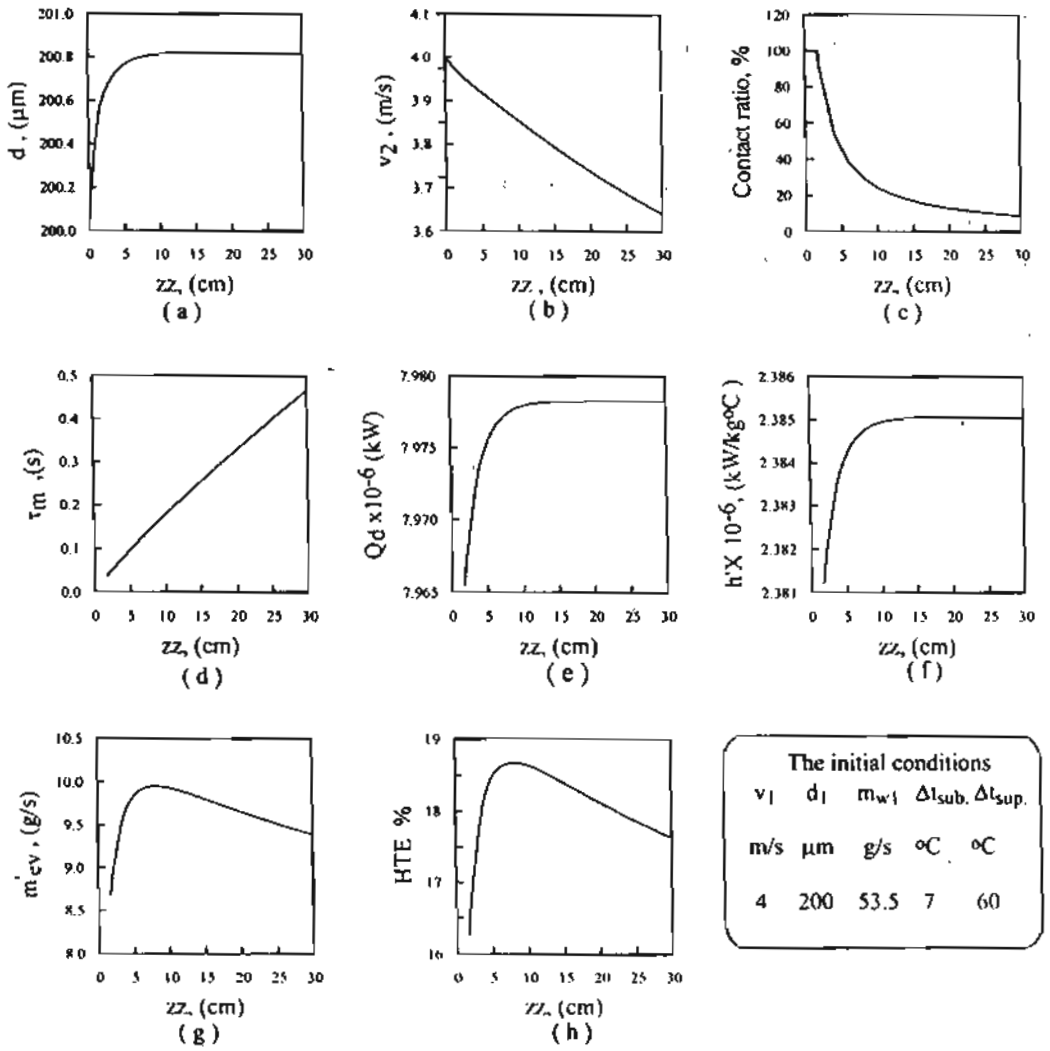


Fig.(5). Effect of the falling distance (*ZZ*) on; a) droplet size, b) droplet velocity, c) contact ratio, d) waiting time, e) transmitted heat per one droplet, f) heat transfer coefficient, g) evaporation rate and h) heat transfer effectiveness.

Figure (5e) illustrates the increase of the transmitted heat from the heated surface per one droplet ($Q_d$) obtained from equation (32) against the falling distance (*ZZ*). From the figure, it can be seen that, this heat is increased by increasing the falling distance. It can also be seen that, the transmitted heat from the heated surface per one droplet increases at a high rate for the low values of the falling distance. That is due to the high rate increasing in the droplet size (d) at the low values of the falling distance. Basically, increasing the droplet size, which allows a large effecting area exposed to the heating surface, increases the transmitted heat from the heated surface per one droplet.

Figure (5f) illustrates the change of heat transfer coefficient (h') obtained from equation (35) against the falling distance (*ZZ*). From the figure, it can be seen that, the heat transfer coefficient is increased by increasing the falling distance. And it can also be seen that, the increasing rate of the heat transfer

coefficient is high at the low values of the falling distance. This is because the droplet size and the transmitted heat per one droplet increase at a high rate at the low values of the falling distance as mentioned in the figures (5a) and (5e). Basically, the heat transfer coefficient is increased by increasing the droplet size and also with the transmitted heat per one droplet.

Figure (5g) illustrates the change of the evaporation rate ($m'_{ev}$) obtained from equation (50) against the falling distance (ZZ). From the figure, it can be observed that, there is a certain value of the falling distance (ZZ) at which the optimum condition for the evaporation process and hence, the maximum evaporation rate occurs. This is because, increasing of the falling distance will result to increase the waiting time ($\tau_m$) and the transmitted heat from the heated surface per one droplet ($Q_d$), as mentioned above. On the other side, the number of droplets in-contact with the heated surface will decrease by increasing the falling distance. Thus, there is a certain value of the falling distance at which the maximum evaporation rate will occur.

Figure (5h) illustrates the change of heat transfer effectiveness (HTE) obtained from equation (53) against the falling distance. Basically the heat transfer effectiveness is directly proportioned to the evaporation rate. Therefore, the effect of the falling distance on the heat transfer effectiveness is the same effect on the evaporation rate. Therefore, as shown in the figure, there is a certain value of the falling distance at which the maximum heat transfer effectiveness will occur. This value is the same value of the falling distance at which the maximum evaporation rate occurs.

3.2. Effect of the droplet initial velocity on the evaporation rate and on the heat transfer effectiveness

To present the effect of the droplet initial velocity ($v_1$) on the evaporation rate and on the heat transfer effectiveness, figure (5) is re-illustrated with various droplet initial velocities of 4, 5 and 6 m/s and with the same working conditions.

Figure (6a) illustrates the effect of the droplet initial velocity on the change of droplet diameter (d) obtained from equation (14). From the figure, at low values of the falling distance (ZZ<15 cm), it can be seen that, the droplet diameter is increased by decreasing the droplet initial velocity. That is because, at low value of the droplet initial velocity, the contact time between the formed vapor and the sprayed droplets is long and hence, the condensation of vapor on the droplet surface is high, so the increasing in the droplet size is high and vice versa. At high values of the falling distance (ZZ >15 cm), the droplet velocity has no effect on the droplet size.

Figure (6b) illustrates the effect of the droplet initial velocity on the droplet velocity ($v_2$). From the figure, it can be seen that, at high droplet initial velocity, the droplet velocity decreases at a high rate. That is because the drag force is increased by increasing the droplet initial velocity.

Figure (6c) illustrates the change of the contact ratio (CR) obtained from equation (28) against the falling distance at various values of droplet initial velocity. From the figure, it can be seen that the droplet initial velocity has no effect on the contact ratio for all values of falling distance.

Figure (6d) illustrates the effect of the droplet initial velocity on the waiting time ($\tau_m$) obtained from equation (48). From the figure, it can be seen that, the waiting time is decreased by increasing the droplet initial velocity. That is because, by increasing the sprayed droplet initial velocity, the horizontal velocity of the droplet on the

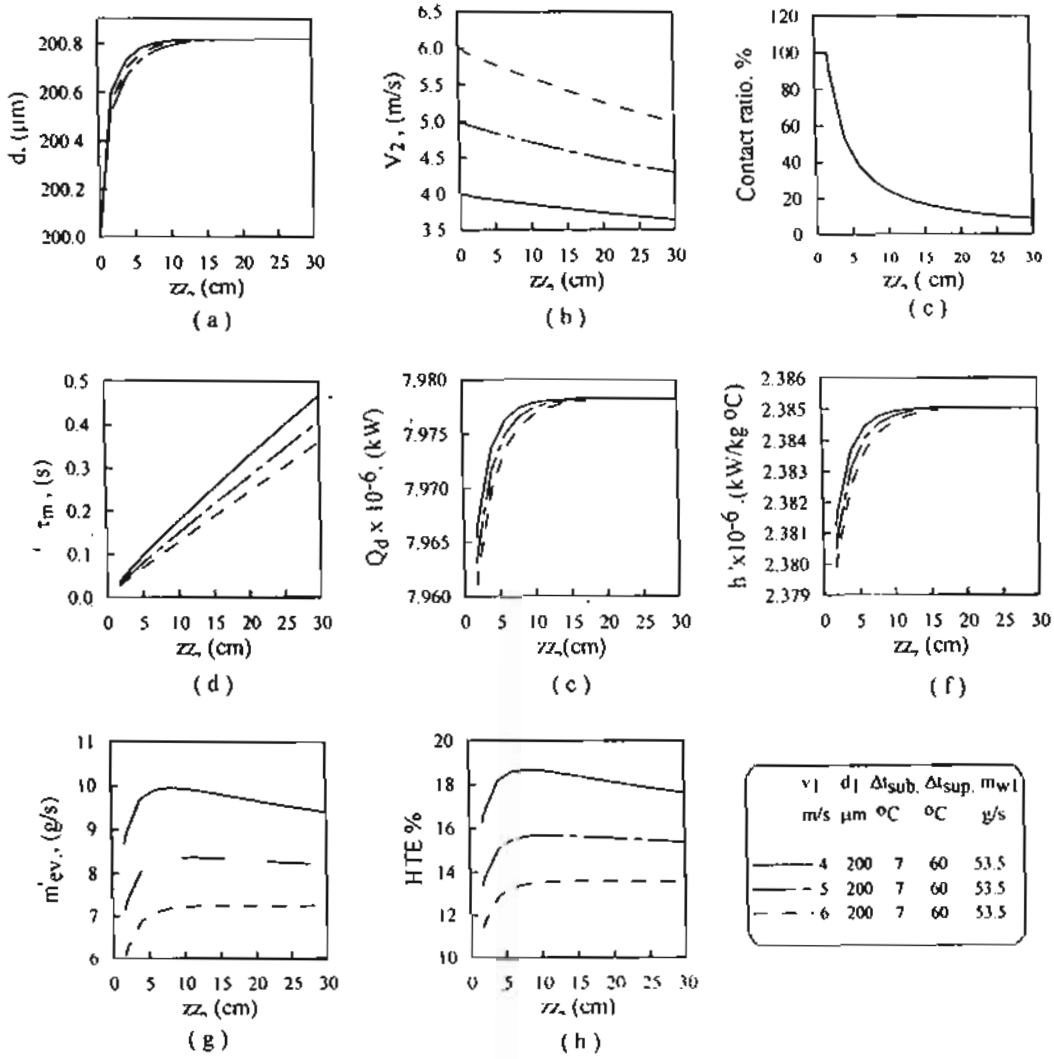


Fig.(6). Effect of the falling distance (ZZ) on: a) droplet size, b) droplet velocity, c) contact ratio, d) waiting time, e) transmitted heat per one droplet, f) heat transfer coefficient, g) evaporation rate and h) heat transfer effectiveness with various initial droplet velocities.

heated tube increases, and hence, the waiting time will decrease. The effect of droplet initial velocity on the waiting time increases with the increase of falling distance.

Figure (6c) illustrates the effect of the droplet initial velocity on the transmitted heat per one droplet ($Q_d$) obtained from equation (32). From the figure, at low values of falling distance ($ZZ$<15cm), the transmitted heat per one droplet decreases by increasing the droplet initial velocity. This is due to the decreasing of the droplet size as mentioned above. At high values of the falling distance ($ZZ$>15cm), the droplet velocity has no effect on the transmitted heat per one droplet.

Figure (6f) illustrates the effect of the droplet initial velocity on the heat transfer coefficient (h') obtained from equation (35). Basically, the transmitted heat per one droplet is increased by increasing the heat transfer coefficient. Therefore, the effects of the falling distance and the droplet initial velocity

on the heat transfer coefficient are the same as their effects on the transmitted heat per one droplet.

Figure (6g) illustrates the effect of the droplet initial velocity on the evaporation rate ($m'_{ev}$) obtained from equation (50). From the figure, it can be seen that, the evaporation rate is decreased by increasing the droplet initial velocity. That is because the waiting time and the transmitted heat per one droplet are decreased by increasing the sprayed droplet velocity, as mentioned above and shown in Figures (6d) and (6e).

Figure (6h) illustrates the effect of the droplet initial velocity on the heat transfer effectiveness (HTE) obtained from equation (53). Basically, the heat transfer effectiveness is increased by increasing the evaporation rate and therefore, the effects of the falling distance and the droplet initial velocity on the heat transfer effectiveness are the same as their effects on the evaporation rate and therefore, the heat transfer effectiveness is decreased by increasing the droplet initial velocity as shown in the figure.

3.3.Effect of the droplet initial diameter on the evaporation rate and on the heat transfer effectiveness

To present the effect of droplet initial diameter ($d_1$) on the evaporation rate and on the heat transfer effectiveness, figure (7) is illustrated with various droplet initial diameters of 0.20, 0.25 and 0.3 mm under the same working conditions.

Figure (7a) illustrates the effect of the droplet initial diameter ($d_1$) on the change of the droplet diameter (d) obtained from equation (14). From the figure, it can be seen that, the droplet size is increased by increasing the droplet initial diameter ($d_1$).

Figure (7b) illustrates the effect of the droplet initial diameter on the droplet velocity ($v_2$). From the figure, it can be seen that, for small droplet initial diameter, there is a high decrease in the droplet velocity in which, for large droplet initial diameter, this decrease is low. This is due to the effect of gravity force. Basically the gravity force is increased by increasing the droplet initial diameter.

Figure (7c) illustrates the effect of the droplet initial diameter on the number of droplets in-contact with the tube surface at various falling distances. Basically, the number of droplets is inversely proportioned to the droplet initial diameter raised to the power three. Therefore, from the figure, it can be seen that, the number of droplets in-contact with the tube surface decreases by increasing the droplet initial diameter.

Figure (7d) illustrates the effect of the droplet initial diameter on the waiting time ($\tau_m$) obtained from equation (48). From the figure, it can be seen that, by increasing the droplet initial diameter, there is a very slight increase in the waiting time. That is because, the large droplet initial diameter, the large exposing area to the heating surface, so a more heat is required for evaporation, where on other side by increasing the droplet initial diameter, the waiting time will decrease due to the increase of the horizontal velocity of the droplet velocity upon the tube surface.

Figure (7e) illustrates the effect of the droplet initial diameter on the transmitted heat per one droplet ($Q_d$) obtained from equation (32). From the figure, it can be seen that, the transmitted heat per one droplet is increased by increasing the droplet initial diameter. That is because, the large droplet initial diameter, the large exposing area to the heating surface and hence, the transmitted heat per one droplet will increase

Figure (7f) illustrates the effect of the droplet initial diameter on the heat

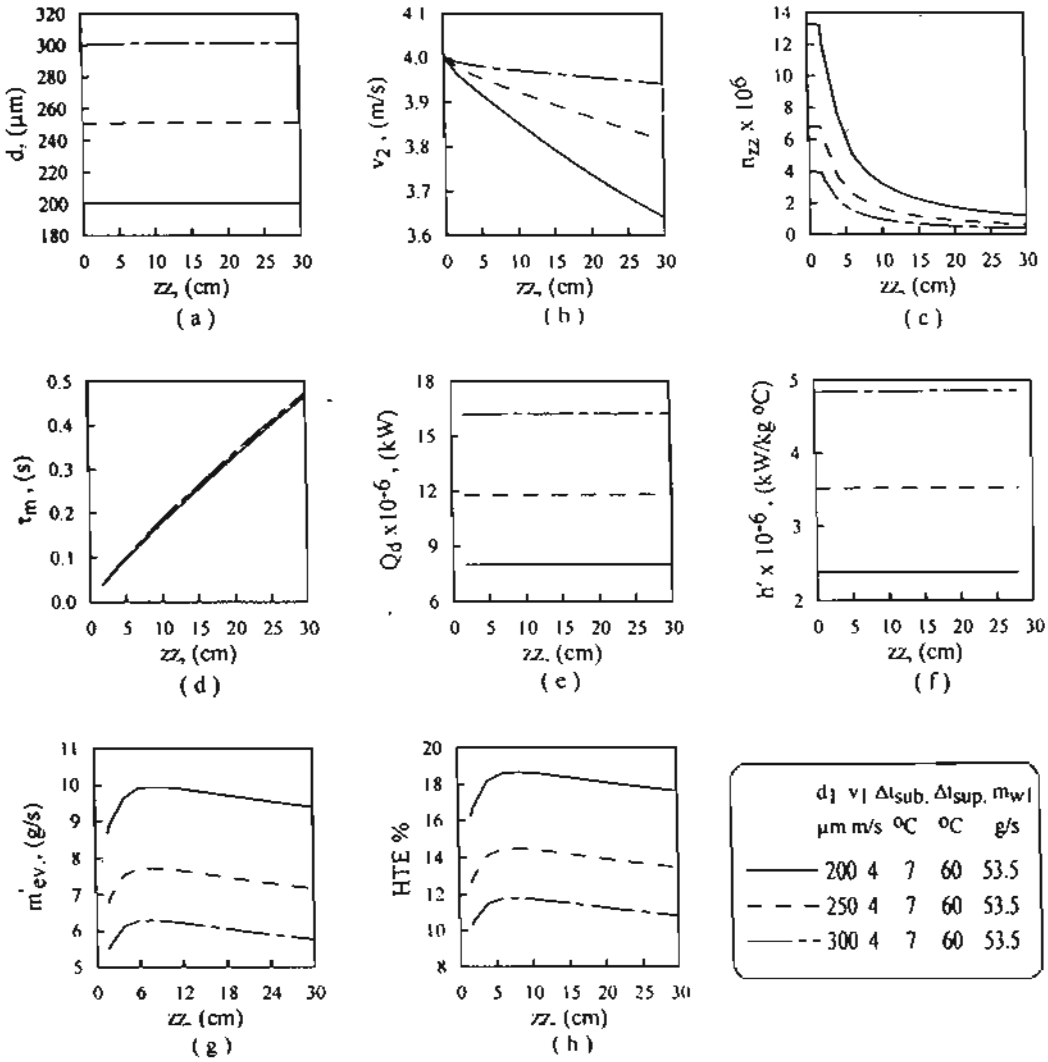


Fig.(7). Effect of the falling distance (ZZ) on; a) droplet size, b) droplet velocity, c) contact number of droplets, d) waiting time, e) transmitted heat per one droplet, f) heat transfer coefficient, g) evaporation rate and h) heat transfer effectiveness with various initial droplet diameters.

transfer coefficient (h') obtained from equation (35). Basically, the transmitted heat per one droplet is increased by increasing the heat transfer coefficient. Therefore, the effect of the droplet initial diameter on the heat transfer coefficient is the same as its effect on the transmitted heat per one droplet, so that, the heat transfer coefficient is increased by increasing the droplet initial diameter.

Figure (7g) illustrates the effect of the droplet initial diameter on the evaporation rate ($m'_{ev}$). From the figure, it can be seen that, the evaporation rate is decreased by increasing the droplet initial diameter, this is due to the decreasing in the number of the sprayed droplets as was shown in fig. (7c).

Figure (7h) illustrates the effect of droplet initial diameter on heat transfer effectiveness (HTE) obtained from equation (53) with the falling distance (ZZ). Basically, the heat transfer effectiveness is increased by increasing the evaporation rate. Therefore, the effects of the falling distance and the droplet initial diameter on the heat

transfer effectiveness are the same as their effects on the evaporation rate. Therefore, the heat transfer effectiveness is decreased by increasing the droplet initial diameter.

3.4. Comparison between the present results and the results obtained by others for the effect of surface superheating on heat flux

Figure (8) shows a comparison between the present results obtained theoretically from equation (49) and the results obtained experimentally by Mousa [13] for the effect of surface superheating temperature on heat flux. From the figure, it can be seen that, the heat flux is increased by increasing the surface superheating temperature. That is because, for the high values of the superheating of the test surface, the temperature difference between the surface temperature and the sprayed droplet temperature is big therefore, a large amount of heat is transmitted from the surface will occur. It can also be seen that, the difference between these results is ranged from 4 to 12 %. That is due to the heat losses to the environment.

3.5. Comparison between the present results and the results obtained by others for the effect of the surface superheating on the heat transfer effectiveness

Figure (9) shows a comparison between the present results obtained theoretically from equation (53) and the results obtained experimentally by Mousa, [13] for the effect of the surface superheating temperature on the heat transfer effectiveness. From the figure, it can be seen that, the heat transfer effectiveness is increased by increasing the surface superheating temperature. That is because, for the high value of the surface superheating, the temperature difference between the test surface temperature and the sprayed droplet temperature is big therefore, a large amount of transmitted heat from the surface will occur. It can also be seen that, the difference between these results is ranged from 4 to 15 %. That is because, the change of droplet mass flow rate, droplet velocity and droplet temperature by increasing the falling distance (i.e. ZZ= 0.57m) is neglected by Mousa [13] in which these changes have a great effect on the evaporation rate and on the heat transfer effectiveness.

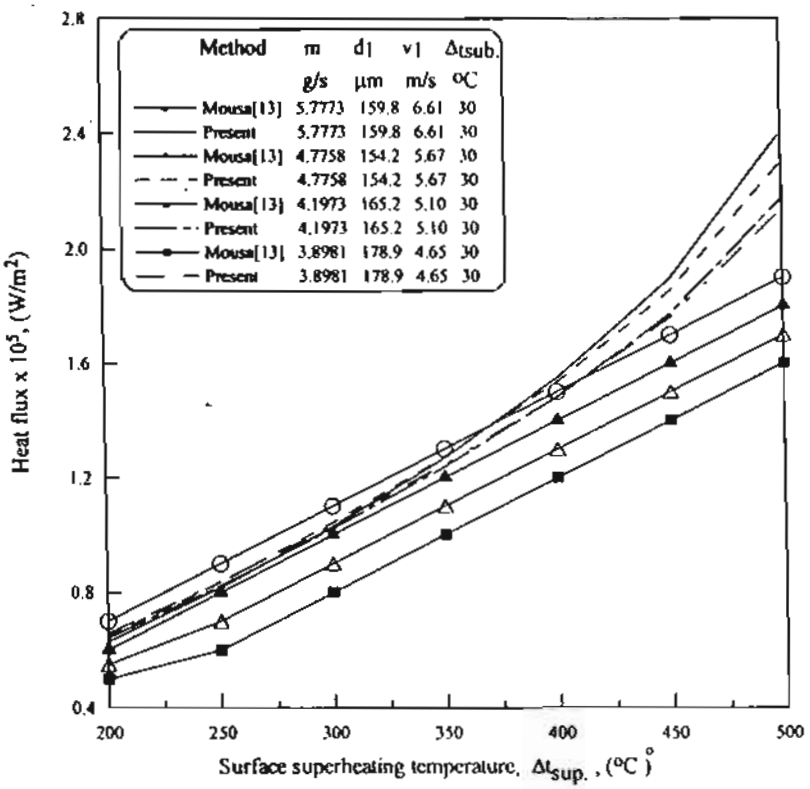


Fig. (8). Comparison between the present results and the results obtained by Mousa [13] for the heat flux against the surface superheating temperature.

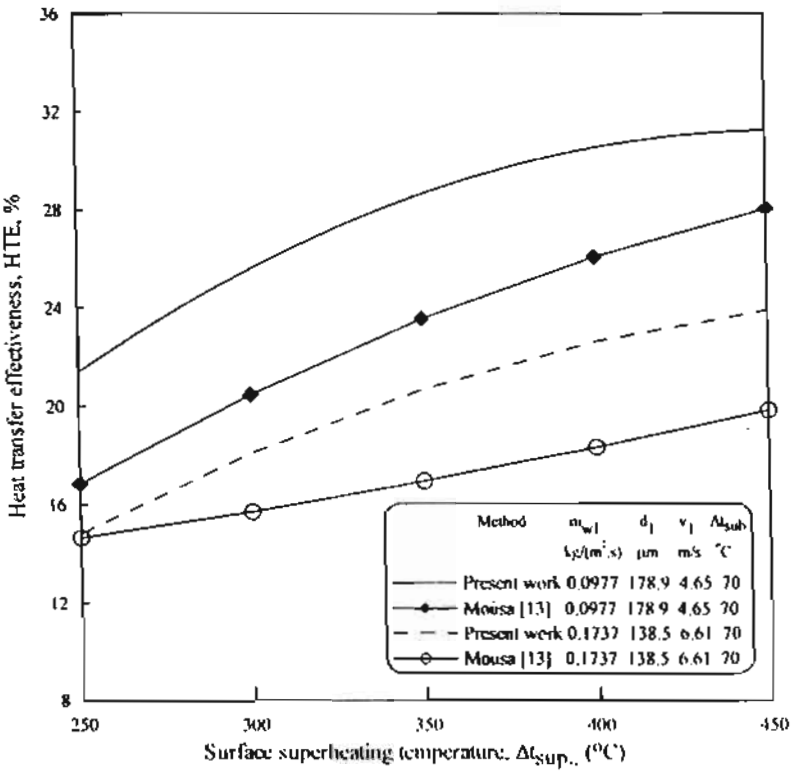


Fig. (9). Comparison between the present results and the results obtained by Mousa [13] for the heat transfer effectiveness against the surface superheating temperature.

**4. Conclusions**

Due to the present study, the following conclusions can be drawn:
There is an optimum distance from nozzle distributor to the hot tube surface at which the maximum evaporation process and hence the maximum evaporation rate will occur. This distance depends on the initial sprayed mass flux, initial droplet velocity, initial droplet size, initial droplet subcooling and the tube surface superheating. The evaporation rate and the heat transfer effectiveness increase by increasing the surface temperature, and also by decreasing the droplet initial velocity. For high initial sprayed mass velocity, the evaporation rate and the heat transfer effectiveness are inversely proportioned to the droplet size. The comparisons between the present results and the experimental data obtained by other researchers are satisfactory.

**References**


1. S. C. Yao, "Analysis on film boiling heat transfer of impacting sprays", Int. J. Heat Mass Transfer, Vol. 32, No. 11, pp. 2099-2112, 1989.
2. Delcorio and K.J. Choi, "Analysis of direct liquid-solid contact heat transfer in mono dispersed spray cooling", J. Thermophysics, Vol. 5, No. 4, pp. 613-620, 1991.
3. Ito, "Studies on the cooling of hot surfaces (Experiment of fog cooling)", Memoirs of the Facility of Engineering, Kyushu University, Vol. 48, No. 3, pp. 211-229, 1988.
4. S. C. Yao and K. J. Choi, "Heat transfer experiments of mono-dispersed vertically impacting sprays ", Int. J. Multiphase Flow, Vol. 13, No. 5, pp. 639-648, 1987.
5. N. A. Ibrahim, "Effectiveness of containment depressurization spray system in nuclear reactors", Ph. D. thesis, Zagazig university, 1989.
6. Jeremy D. M. Linn, Stephen, J. Maskell and Mike A. Patrick, "A Note on heat and mass Transfer to a spray droplet", Nuclear Technology, Vol. 81, pp. 122-125, APR. 1988.
7. I.S. Lim, R. S. Tankin and M. C. Yuen, "Condensation measurement of horizontal steam/water flow", Journal of Heat Transfer, Vol. 106, pp. 425-482, May 1984.
8. A. Lekic and J. D. Ford, "Direct contact concentration of vapor on a spray of subcooled liquid droplets ", Int. J. Heat Mass Transfer, Vol. 23, pp. 1531-1537, 1980.
9. J. Baumeister and T. D. Hamil, "Creeping flow solution of the leidenfrost phenomenon", NASA TN D-3133, 1965 .
10. Ito, "On the water cooling of hot surfaces-analysis of fog cooling in the region associated with film Boiling", Proceeding of the ICHMT International Symposium on Manufacturing and Materials Processing, Dubronik, August, 1990.
11. Lin Jie Huang and P. S. Ayyaswamy, "Heat and mass transfer associated with a spray drop experiencing condensation: a fully transient analysis", Int. J. Heat Mass Transfer, Vol. , No. 5, pp. 881-891, 1987.
12. El-Sayed R. Negeed, "Experimental and computational investigation of spray heat exchanger performance", Ms. C. Thesis, Mansoura university, Egypt, 1998.
13. Mousa M. Mousa, "Studies on the water cooling of hot surfaces", Ph. D. Thesis, Kyushu University, Kukuoka, Japan July 1992.